Journal of Pharmaceutical Innovation (2019) 14:112–122
https://doi.org/10.1007/s12247-018-9335-z

ORIGINAL ARTICLE

Hydrogel Containing PEG-Coated Fluconazole Nanoparticles with Enhanced Solubility and Antifungal Activity

Ahmed A. H. Abdellatif[1,2] · Dalia Farag A. El-Telbany[3] · Gamal Zayed[1,4] · Majid M. Al-Sawahli[5]

Published online: 6 July 2018

Abstract

Purpose The aim of this study was to prepare fluconazole (FLC) nanoparticles coated with polyethylene glycol (PEG) in the form of FLC-PEG-NPs and optimize the size and entrapment efficiency.

Methods Nine formulae were prepared by solvent antisolvent precipitation technique according to full 3^2 factorial designs. The effects of PEG molecular weight (X_1) and the drug polymer ratio (X_2) on the particle size (Y_1) and entrapment efficiency (Y_2) were explored. The prepared FLC-PEG-NPs were investigated for particle size, count rate, PDI, zeta potential, and morphology. Carbopol hydrogel was prepared, loaded with optimized FLC-PEG-NPs, and characterized for pH, FLC content, viscosity, homogeneity and spreadability, in vitro release, skin permeation, and antifungal activity.

Results The formulated nanoparticles were uniform in size and spherical in shape with slightly rough surface and free from aggregations. The effect of PEG molecular was antagonistic on the particle size and was agonistic on EE %. The release of drug from hydrogel containing pure FLC was always lower than that from hydrogel containing FLC-PEG-NPs. The kinetic analysis of drug release obeys first-order release model and super case II transport mechanism. The cumulative amount of drug permeated applying hydrogel containing optimized FLC-PEG-NPs was significantly higher than the amount permeated using pure fluconazole containing hydrogel. The antifungal activity of hydrogel containing FLC in the form of optimized PEG-coated nanoparticles was better than hydrogel containing pure drug as indicated by relatively high inhibition zone using agar well-diffusion method.

Conclusion Small spherical FLC nanoparticles with enhanced in vitro drug release as well as improved antifungal activity could be achieved by using PEG-coated fluconazole nanoparticles.

Keywords Fluconazole · Polyethylene glycol · Nanoparticles · Skin permeation

Introduction

Solubility enhancement of poor water-soluble drug is an important factor in preparing effective dosage form that can be either administered systemically or applied locally. The size and morphology of the drug affect the biopharmaceutical properties such as solubility, dissolution rate, and absorption rates. Solid dispersion, inclusion complexation, nanoparticles, and nanosuspension are the most extensively applied methods for improving drug solubility, stability, and bioavailability of active ingredients. The increased drug solubility by nanoparticles is attributed to the decreased particle size with subsequent increase in the surface area. However, it is necessary to report certain disadvantages of nanoparticles such the tendency for aggregation in biological systems due to high surface energy, short biological half-life, and high risk of toxicity either acute or chronic [1–6].

Nanonization is the preparation of ultrafine nanoparticles by solvent evaporation. Nanonization is a simple, rapid, and low-cost method for enhancing the solubility and dissolution rate of poorly soluble drugs [3]. Recently, nanoprecipitation is an alternative method that is widely applied for nanoparticle

✉ Gamal Zayed
gamalzayed@hotmail.com

1 Department of Pharmaceutics and Industrial Pharmacy, Faculty of Pharmacy, Al-Azhar University, Assiut, Egypt.

2 Department of Pharmaceutics, College of Pharmacy, Qassim University, 51452 Al Qassim, Kingdom of Saudi Arabia

3 Department of Pharmaceutics, Faculty of Pharmacy, October University for Modern Sciences and Arts (MSA), Cairo, Egypt.

4 Al-Azhar Centre of Nanosciences and Applications (ACNA), Al-Azhar University, Assiut, Egypt.

5 Department of Pharmaceutical Technology, Faculty of Pharmacy, Kafrelsheikh University, Kafrelsheikh, Egypt.

preparation to enhance dissolution and improve the bioavailability of poor water-soluble drug. This technique depends on the solubility difference of the drug between a solvent and antisolvent. This could be explained by the fact that the drug is highly soluble in one solvent (organic solvent) which is miscible with the antisolvent (water). After addition of non-aqueous solution of the drug to water and allowing the evaporation of the organic solvent by stirring and/or heating, the water-insoluble drug will be precipitated in the aqueous phase in the form of small nanoparticles. The presence of water-soluble stabilizers such as PEG, PVP, and sodium carboxymethyl cellulose is essential in obtaining nanoparticles with small size and improved solubility. These stabilizers help prevent the drug crystal growth after solvent evaporation and finally coat the obtained nanoparticles with a hydrophilic corona of stabilizer leading to the formation of small drug particles with high water solubility [4].

Polyethylene glycol (PEG) is a well-known non-toxic and biocompatible polymer with many applications in the pharmaceutical fields. The polymer is characterized by high biocompatibility, high water solubility, and adherence of its molecules to nanoparticle surface (PEGylation) which decreases nanoparticle aggregation by steric stabilization, enhances water solubility of the drug, and reduces the size of the produced nanocomposites [7].

Fluconazole is a potent and broad-spectrum antifungal agent used for the treatment of systemic as well as the superficial fungal infections. The poor water solubility and severe side effects limit the bioavailability, therapeutic efficacy, and local delivery of the drug [8].

Accordingly, the aim of the current study is to enhance water the solubility of fluconazole, as a preliminary step, for producing effective topical gel preparations of the drug. A new method for improving water solubility has been applied which depends on the formation of fluconazole nanoparticles in the presence of PEG molecules using solvent antisolvent techniques. Furthermore, the produced FLC-PEG-NPs have been incorporated into Carbopol 940 gel bases for investigation of antifungal activity of fluconazole nanoparticles.

Experimental

Materials

FLC was kindly supplied from EIPICO Pharmaceutical Company, Cairo, Egypt. Different molecular weights polyethylene glycols (PEG 4000, 10,000 and 20,000) were purchased from Fluka Chemical Company, Germany. Methanol was obtained from El Nasr Chemical Co. (Abu Zaabal, Egypt). Carbopol 940 and cellophane membrane (molecular weight cutoff 140 kDa) were purchased from Sigma-Aldrich Chemical Co., Germany. All other chemicals and solvents were of analytical grade. FLC-PEG-NPs were prepared in the laboratory of Pharmaceutics Department, Faculty of Pharmacy, Al Azhar University, Assiut, Egypt.

Methods

Factorial Design and Preparation of FLC-PEG-NPs

The application of a factorial design gives a statistically systematic approach for the preparation and optimization of nanoparticles with desired particle size, polydispersity index, and loading efficiency. A full 3^2 factorial design was constructed in this study using Minitab software (USA). The studied factors were molecular weight (X_1) and drug polymer ratio (X_2). Three levels, low, medium, and high, for each variable were determined. The design aimed to study the combined effect of these factors on the particle size (Y_1), and the entrapment efficiency (Y_2). Mathematical equations were used to correlate each response to the factors affecting it. Counterplots and response surface plots were constructed and an optimum formulation was selected using the desirability function [9–11].

Nine experimental runs were developed as indicated in Table 1. Each run was carried out in triplicate to assure accuracy and reproducibility. FLC nanoparticles were prepared and coated with PEG by applying solvent antisolvent precipitation method as reported with slight modification [4, 12]. The calculated amount (200 mg) of the drug and polymer was dissolved in 10 ml of ethanol (solvent) and added dropwise to 50 ml of polymer aqueous solution (antisolvent) stirred at 50 rpm for 30 min. Different weight ratios of drug to polymer, namely, 1:1, 1:2, and 1:3, and different molecular weights of PEG (4000, 10,000, and 20,000) were employed. The final obtained FLC-PEG-NPs were purified by filtration using a Whatman filter paper No. 42 to remove large aggregates. The method of preparing FLC-PEG-NPs is represented in Fig. 1.

Table 1 Experimental runs exhibiting formulation factors

Run	Factors	
	X_1	X_2
F1	4000	1:1
F2	4000	1:2
F3	4000	1:3
F4	10,000	1:1
F5	10,000	1:2
F6	10,000	1:3
F7	20,000	1:1
F8	20,000	1:2
F9	20,000	1:3

X_1 molecular weight of PEG; X_2 drug polymer ratio

Determination of Size, Count Rate, Polydispersity Index, and Zeta Potential

Dynamic light scattering (DLS) was utilized to determine the particle size, count rate, and polydispersity index (PDI) of FLC-PEG-NPs. One milliliter of each sample was considered for measuring in a disposable cuvette in three tentative replicates. The samples were subjected to laser light with an occurrence laser beam of 633 nm and a scattering angle of 90° at room temperature [13].

Entrapment Efficiency Percent

The percentage entrapment efficiency (EE%) of FLC in the prepared FLC-PEG-NP formulations was performed as reported [14]. Briefly, 1 ml sample was centrifuged at 14,000 rpm (Centurion, Scientific Ltd., UK) for 60 min at 4 °C. The supernatant was separated from the precipitated nanoparticles which were washed twice with phosphate-buffered saline (PBS) of pH 7.4. Then, the clear fraction (supernatant) was collected and assayed for the free unentrapped drug. The amount of unentrapped *FLC* was determined, in the collected supernatant, by UV-visible spectroscopy at λ_{max} 260 nm (Shimadzu-1700 UV, Japan) [8].

$$\text{EE } \% = \frac{\text{Total drug concentration-Concentration of drug in the supernatant}}{\text{Total drug concentration}} \times 100 \quad (1)$$

Surface Morphology of Nanoparticles

The surface morphology of plain PEG and FLC-PEG-NPs was examined using SEM instrument operated at 4–25 kV on samples gold-sputtered for 120 s at 10 mA under argon gas and low pressure [15, 16].

FT-IR Spectroscopy

The presence of PEG molecules on the particle surfaces was detected using Fourier transform infrared spectrophotometer (FTIR). Samples of pure drug, pure polymer, and FLC-PEG-NPs were scanned in the range from 400 to 4000 cm^{-1}. The data were recorded on a FTIR (SSP-10 A Shimadzu Co., Japan), using the KBr disk technique [15].

Preparation of FLC-PEG-NP Hydrogel

Carbopol 940 polymer hydrogels, containing 1% of pure drug or the equivalent amount of optimized FLC-PEG-NP formula, were prepared by the previously stated method [14]. Briefly, Carbopol 940 (1%, *w*/*v*) was added step by step to a beaker holding an aqueous suspension of either pure FLC or FLC-PEG-NPs with constant stirring until a homogenous gel is produced. After that, sodium hydroxide (0.4%, *w*/*v*) was added to neutralize the free acid liberated from Carbopol 940.

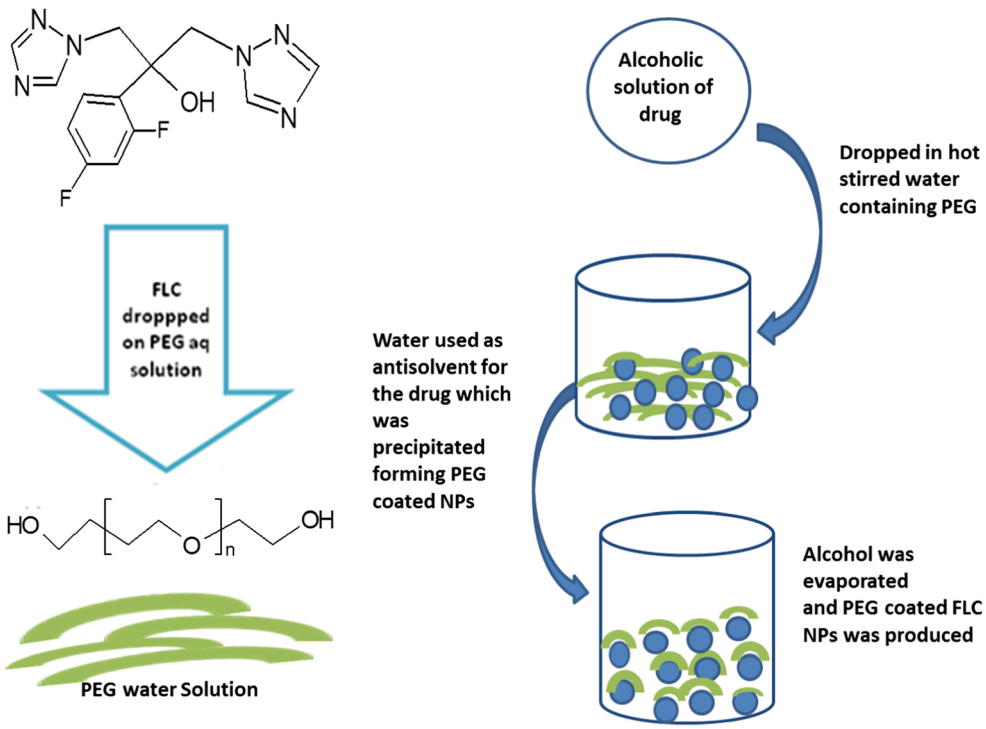

Fig. 1 Preparation of PEG-coated fluconazole nanoparticles (FLC-PEG-NPs)

Evaluation of FLC-PEG-NP Hydrogel

Determination of pH and FLC Content of the Hydrogel The pH values of pure drug hydrogel and optimized FLC-PEG-NP hydrogel were estimated using a digital pH meter.

For determination of drug content, fluconazole was first extracted from hydrogel by ethyl alcohol. Briefly, 100 ml of ethanol was added to 100 mg of hydrogel into a beaker and sonicated for 15 min. Later, the ethanolic extract was purified by filtration using a Whatman No. 44 filter paper. The drug content (%) in hydrogel formulations was determined as mentioned in section "Entrapment efficiency percent" [8].

Rheological Behavior and Viscosity Measurement of FLC-PEG-NP Hydrogel The viscosity of the prepared hydrogel was measured at different angular velocities using spindle No. 4. Pure FLU-PEG-NPs and FLC-PEG-NP hydrogel were estimated for their rheological activities by rheometer instrument using cone and plate pattern. The rheometer was set with cone-plate geometry (4/40) working in the oscillation mode. The hydrogel samples were located onto the bottom plate of the rheometer, then, the upper plate was lowered to a gap size of 1000 μm. Viscosities were determined at 27 °C and 1 Hz oscillatory frequency as a function of the applied stress [14].

Homogeneity Test and Spreadability The homogeneity of a plain hydrogel and FLC-PEG-NP hydrogel was examined by visual inspection of a number of samples ($n = 5$) of the hydrogels. A small magnitude of each hydrogel sample is hard-pressed between the thumb and the index finger to observe the uniformity of the hydrogel whether homogeneous or not. The spreadability of the gel formulation was determined by measuring the diameter of 1 g hydrogel placed between horizontal plates (20×20 cm^2) after 1 min of application of standardized weight (125 g) on the upper plate.

In Vitro Release of Drug from the Prepared Hydrogel and Kinetic Analysis of Drug Release

In vitro FLC release of FLC-PEG-NP hydrogel of optimized formula has been investigated using a release cell resembling Franz diffusion cell. In brief, a wetted cellophane membrane was stretched out over the end of an open-ended glass tube and made watertight using a rubber band. Hydrogel containing FLC equivalent to 20 mg was placed into the glass tube above the cellophane membrane (donor compartment). The tubes were immersed vertically in a 100-ml beaker containing phosphate buffer, 50 ml (pH 7.4, 10 mM) maintained in a thermostatically controlled shaker (50 rpm) at 37 °C (receptor compartment). At predetermined time intervals for up to 12 h, 5 ml aliquots of the release medium were withdrawn from the receptor compartment and replaced with equal volume of fresh phosphate buffer to hold the volume of release medium constant. FLC content in the withdrawn samples was determined spectrometrically as previously described [17].

The data obtained from in vitro release studies were fitted to various kinetic models such as zero order, first order, and Higuchi's model in order to determine the release kinetic profiles. Moreover, Korsmeyer-Peppas model as the logarithm of cumulative percentage of FLC released versus the logarithm of time (log time) was used to determine the mechanism of FLC release. Then, slope of the produced straight line could be used to calculate the value of the exponent (n). The relations were used to interpret the result outputs as follows: if the n equals to 0.5, the diffusion mechanism is Fickian (as in the case with slab matrix system); if n is larger than 0.5 and less than 1, the diffusion mechanism is non-Fickian; if n equals to 1, that refers to a case II relaxational transport; and finally if n more than 1, to super case II transport.

Ex Vivo Permeation Study of FLC-PEG-NP Hydrogel Using Abdominal Skin of Rat

The permeated and cumulative amounts of FLC across rat abdominal skin treated with optimized FLC-PEG-NPs, FLC-PEG-NP hydrogel as well as control hydrogel (containing pure FLC) after 12 h was determined. Control hydrogel (containing pure FLC) and FLC-PEG-NP hydrogel were applied on two different groups of rats. The statistical difference was investigated using one-way ANOVA followed by Tukey's post hoc test at probability (p) < 0.05. Permeation study of FLC was conducted using abdominal male rat (weighed 140 ± 20 g) skin [17]. The rats were first sacrificed and their hair was removed from the dorsal side of the rat using 0.1-mm hair clipper to develop the fresh skin of the rats. A wet cotton swab soaked in isopropanol was used to wipe the dermal part of the skin for any remaining fat materials. Skin turned out to be saturated with phosphate buffer before permeation study by soaking them in phosphate buffer for 6 h. Skin portion was strained over one end of an open-ended glass tube, then immersed in a 400-ml beaker holding 125 ml of the buffer and held in vertical situation so that the skin was just under the surface of the buffer solution. The tube (donor) and beaker (acceptor) were kept at 37 °C in thermostatically controlled shaker water bath. The donor chamber was loaded with 1 gram of hydrogel (containing 100 mg FLC). At various time intervals (up to 24 h), samples of 2.0 ml were removed from the receptor and replaced with phosphate buffer. Each experiment was repeated three times and FLC content in

Fig. 2 Particle size, count rate, and polydispersity index and zeta potential of factorial design runs

a) F1
Average diameter 943.9 ± 80.86 nm. One peak with 100% intensity; PDI value of 0.480. Zeta potential of 33.4 mV.

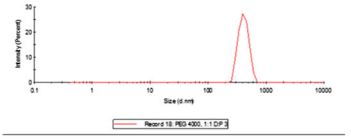

b) F2
Average diameter 858.6 ± 73.8 nm. One peak with 100% intensity; PDI value of 0.769. Zeta potential of 27.5 mV.

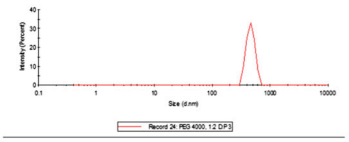

c) F3
Average diameter 951.4 ± 55.63 nm. One peak with 100% intensity; PDI value of 0.764. Zeta potential of 31.2 mV.

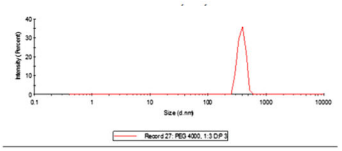

d) F4
Average diameter 527.2 ± 237.7 nm. One peak with 100% intensity; PDI value of 0.668. Zeta potential of 29.6 mV.

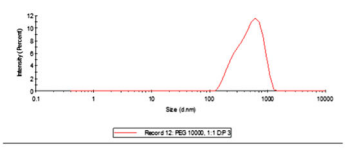

e) F5
Average diameter 560.7 ± 93.35 nm. One peak with 100% intensity; PDI value of 0.582. Zeta potential of 37.7 mV.

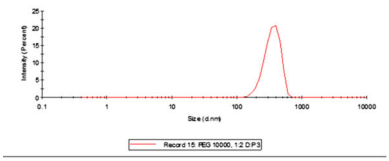

f) F6
The first peak with intensity of 85% and average diameter of 591.1 ± 240.8 nm. The second peak 9.639 nm and 8.6% intensity. The third 5365 ± 333.5 with intensity 6.4%; PDI value of 0.965. Zeta potential of 36.2 mV.

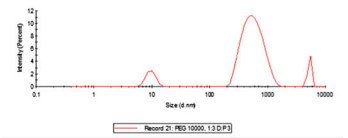

g) F7
Average diameter 317.7 ± 37.49 nm. One peak with 100% intensity; PDI value of 0.658. Zeta potential of 39.8 mV.

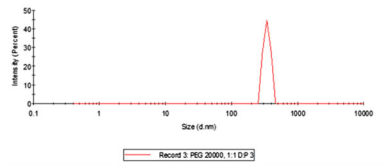

h) F8
Two peaks; one Peak with intensity of 95% and average diameter is 261.6 ± 49.55 nm. The second peak 7.564 ± 0.6215 nm of 5% intensity; PDI value of 0.863. Zeta potential of 41.2 mV.

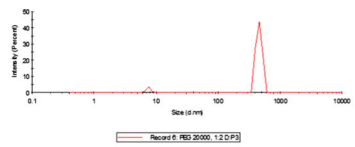

i) F9
Average diameter 286.4 ± 47.55. One peak with 100% intensity; PDI value of 1. Zeta potential of 38.8 mV.

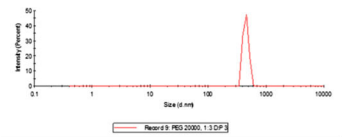

the withdrawn samples was determined spectrophotometrically at 260 nm [14].

The flux (J) was obtained from the slope of the linear line obtained by plotting the cumulative permeated amount per

unit area versus time. Also, the percutaneous permeability coefficient (K_p) of FLC across the abdominal rat skin was estimated using Fick's first law of diffusion and expressed by the following equation:

$$K_p = \frac{J}{C} \quad (2)$$

Where; J is the flux (mg/cm^2/h) and C is the total FLC concentration in donor partition.

Antifungal Activities

Different strains of fungi were used to study the antifungal activity of FLC powder (positive control) and FLC-loaded hydrogel (tested formula) using agar well-diffusion method. Sterile filter discs impregnated with FLC solution or the equivalent amount of hydrogel were placed on the agar plates. The concentration of both tested formulae was 25 μg per disc of pure drug or hydrogel. The diameters of inhibition zone were measured in millimeters after 2 days of incubation at 37 °C [18].

Results and Discussion

Factorial Design and Preparation of FLC Nanoparticles

In the current study, hydrophilic PEG was utilized as a coating material to enhance the aqueous solubility of FLC applying the precipitation method. The methanolic solution of drug was added to vigorously stirred water containing the dissolved polymer at room temperature. FLC-PEG-NPs were obtained after evaporation of methanol. The solution was gradually changed from clear solution to cloudy indicating the formation of highly dispersed FLC-PEG-NPs. Particle size, count rate, PDI, and zeta potential were used to confirm nanoparticle formation and also were used as parameters that indicate the dispersion stability of FLC-PEG-NPs [19, 20].

Determination of Particle Size, Count Rate, and Polydispersity Index and Zeta Potential

The polydispersity index (PDI) is a measure of the size distribution of polymer molecular weights and colloidal systems and also considered as an index that could indicate the dispersion stability of nanoparticles. High PDI values indicate the heterogeneity of the nanoparticle size (particles of different sizes) in suspension, while smaller PDI indicates the homogeneity of the nanoparticle size (monodisperse nanoparticles) in suspension. In the present study, the values of PDI record a range from 0.48 to 0.965 (as shown in Fig. 2). Ideally, the value of PDI should be less than 0.70

Table 2 Experimental runs exhibiting formulation factors

Run	Responses	
	Y_1	Y_2
F1	943.9	76.5
F2	858.6	79.45
F3	951.4	72.85
F4	527.2	80.5
F5	560.7	85.05
F6	591.1	82.25
F7	317.7	95.01
F8	261.5	91.72
F9	286.2	89.39

Y_1 mean particle size (nm); Y_2 entrapment efficiency (%)

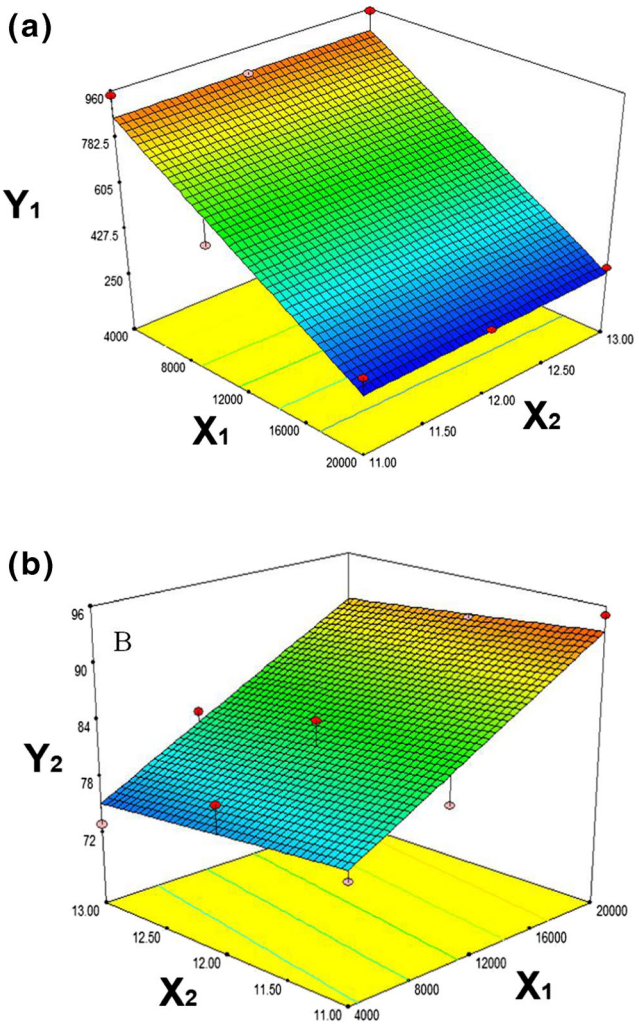

Fig. 3 Three-dimensional surface response plot showing the effect of polymer molecular weight and drug polymer ratio on the particle size (**a**) and entrapment efficiency (**b**). X_1, molecular weight of PEG; X_2, drug polymer ratio; Y_1, mean particle size (nm); Y_2, entrapment efficiency (%)

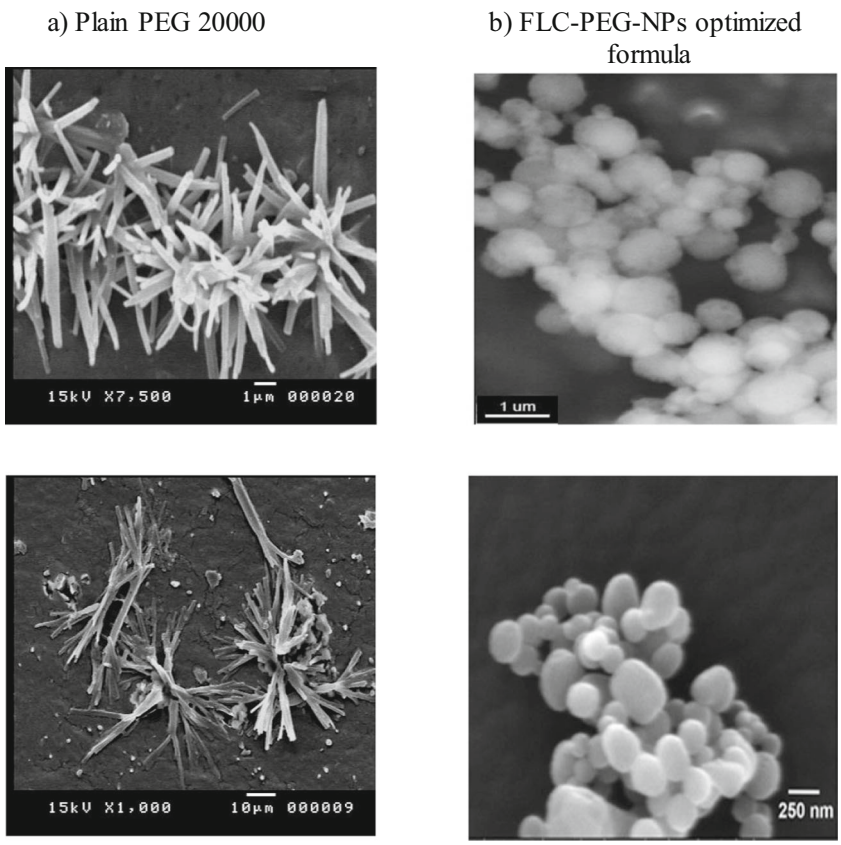

Fig. 4 SEM images for plain PEG 20000 and FLC-PEG-NP optimized formula

because this value indicates narrow size distribution of particles, i.e., monodisperse colloidal system [21].

Zeta potential of the prepared formulations exhibited a range of 27.5 to 41.2 mV which indicates stability of the

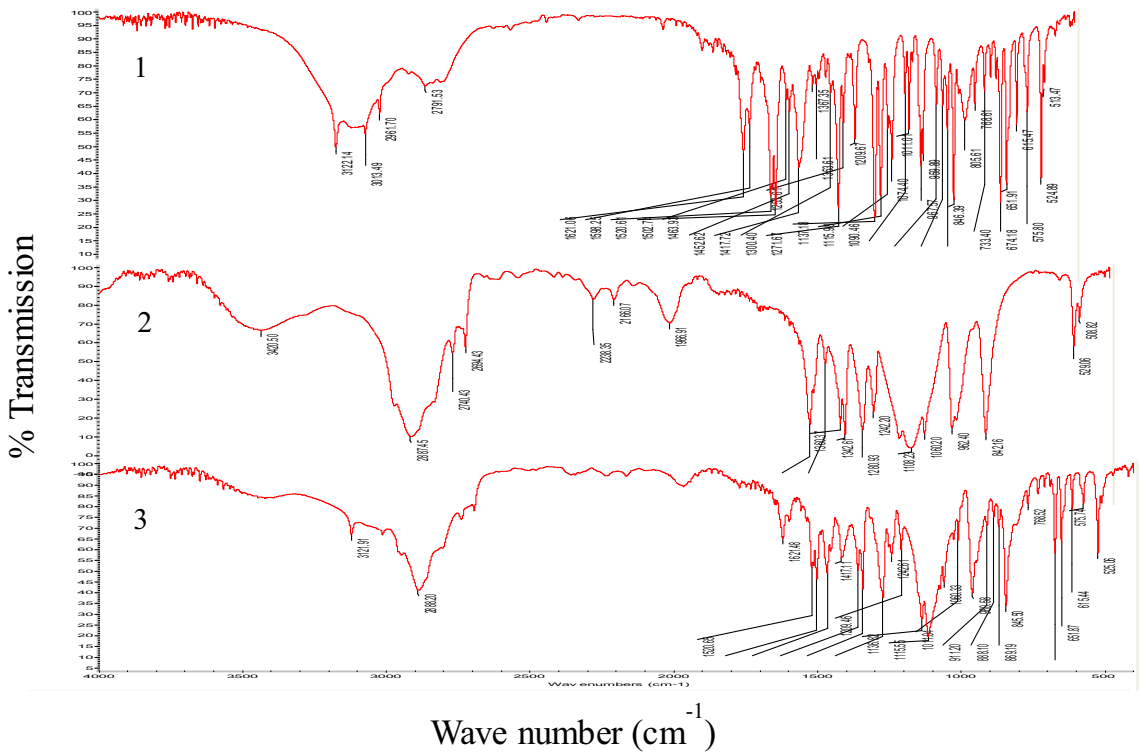

Fig. 5 FT-IR spectra of pure fluconazole (1), pure PEG 20000 (2), and optimized FLC-PEG-NPs (3)

Table 3 The pH, entrapment efficiency, viscosity, homogeneity, spreadability of plain hydrogel, and optimized FLC-PEG-NP hydrogel formulations

Formulation	pH	FLC content	Viscosity (cPs)	Homogeneity	Spreadability (g cm/s)
Plain hydrogel	7.1 ± 0.4	Nil	4517 ± 63	Good	7.65 ± 0.45
FLC-PEG-NP hydrogel	6.8 ± 0.3	98.88 ± 3.9	4998 ± 99	Good	6.4 ± 0.5

systems. Zeta potential refers to the degree of electrostatic repulsion of the dispersed system. Higher zeta potential values indicate stability of dispersion and its resistance to aggregation [21].

According to full 3^2 factorial designs, the factor combinations yielded various values of observed dependent variables. The results of average particle size (Y_1) were 261.5 and 951.4 nm for runs 8 and 3, respectively (Table 2). The entrapment efficiency (Y_2) showed a highest value of 95.01% (run 7) and a lowest value of 72.85% (run 3). The effects of independent variables, polymer molecular weight (X_1), and drug polymer ratio (X_2), on the responses, particle size (Y_1) and entrapment efficiency (Y_2), are indicated in Fig. 3. For the optimized formulation of FLC nanoparticles, the particle size should be lowest and the entrapment efficiency should be highest. As shown in Fig. 3a, the particle size decreases with increasing the molecular weight of PEG (X_1) and not affected by the used amount of the polymer (X_2). This result could be attributed to the increased viscosity of the antisolvent (water) by increasing polymer molecular weight and inhibition of nanoparticle growth during solvent evaporation leading to the formation of small nanoparticles. The increased amount and molecular weight of the used polymer could also reduce the chance of nanoparticle aggregation by the formation of hydrophilic coat around the formed nanoparticles [22, 23] .

Regarding the entrapment efficiency, a high positive effect is observed with (X_1) and a minor positive effect is observed with (X_2). The increased entrapment with increasing molecular weight could be attributed to higher viscosity. In contrast, the low molecular weights (4000 and 1000 Da) are not able to increase the viscosity of water (antisolvent) enough and consequently some of the drug would be precipitated in the microcrystals form which could be removed by filtration leading to lower entrapment efficiency.

The mathematical modeling of PEG-coated fluconazole nanoparticles was carried out by Eqs. (3) and (4):

$$P.S = 1549.02 - 0.0593312X_1 - 2217.4X_2 + 6.8046910^{-7}X_1{}^2 + 0.00975\ X_1\ X_2 + 2729.6\ X_2{}^2 \quad (3)$$

$$EE = 50.5824 + 0.000218646X_1 + 131.637X_2 + 2.4270810^{-8}\ X_1{}^2 + 0.0004925\ X_1\ X_2 - 170.027\ X_2{}^2 \quad (4)$$

After analyzing the effect of independent variables on dependent variables, the level of factors was specified using computerized optimization. Accordingly, the predicted values of Y_1 and Y_2 were 254.3 nm and 93.7%, respectively. These predicted values were deduced at X_1 and X_2 of 20,000 and 1:1.43, respectively. To confirm the output predictions, a fresh formulation of FLC-PEG-NPs was formulated using the specific optimized values. These optimized levels yielded a new formulation with a particle size of 266 nm and entrapment efficiency of 95.1%. The close agreement of the observed and predicted values exhibited the reliability of the optimization procedure.

Surface Morphology of Nanoparticles

In order to prove the formulation of FLC-PEG-NPs, the plain polymer and optimized formula were scanned by SEM. SEM imaging of used polymer alone showed an irregular structure which could not be identified as nanoparticles (Fig. 4a). However, SEM examination identified and confirmed FLC-PEG-NP formation (Fig. 4b).

FLC nanoparticles formed using PEG as a coat were mostly homogeneous, spherical and free from aggregates as presented in Fig. 4b. Under higher magnification power, the surface of the FLC-PEG-NPs was slightly rough. This

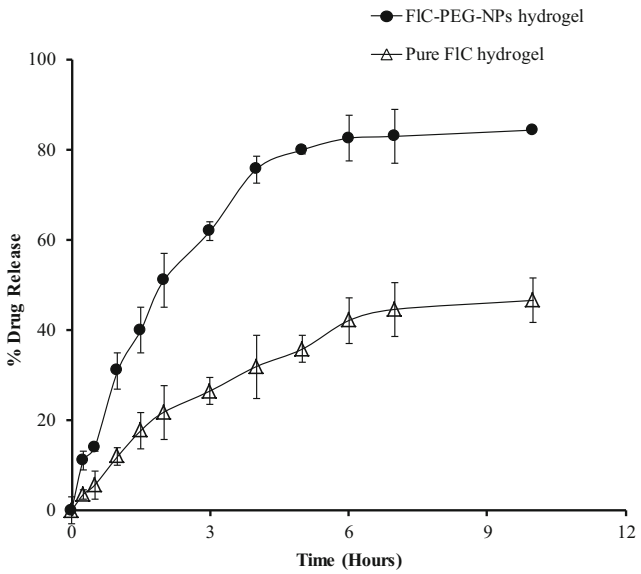

Fig. 6 In vitro drug release from optimized FLC-PEG-NP hydrogel and pure FLC hydrogel

Table 4 Kinetic release data of FLC from pure FLC and FLC-PEG-NP-loaded hydrogels

Formula	Correlation coefficient (R^2)		Release rate constant (K)	
	Pure FLC	Optimized formula	Pure FLC	Optimized formula
Zero	0.965	0.961	9.163	20.837
First	0.977	0.993	0.107	0.327
Higuchi	0.954	0.966	16.567	37.975

observation may be due to the higher concentration of drug in the optimized formula that dispersed at the molecular level. The adhesion of nanoparticles together as indicated in Fig. 4b is due to the drying of nanoparticles before examination by SEM which showed different shapes for nanoparticles adhered together. On the other hand, these nanoparticles could not be identified by transmission electron microscope (TEM) due to the lack of high electron density and the weak contrasting ability of the PEG outer layer around the nanoparticles [24].

FT-IR

Figure 5 shows the IR spectra of fluconazole, PEG, and FLC-PEG-NPs. The spectrum of pure drug is characterized by IR peaks at 1520, 1598, 1621, 3000, and 3120 cm^{-1}. The spectrum of PEG is characterized by peaks at 1996, 2238, 2695, 2740, 2887, and 3420 cm^{-1}, while the spectrum of FLC-PEG-NPs shows the characteristic peaks of both drug and polymer which prove the presence of PEG on the particle surface and also prove the absence of chemical interaction between FLC and PEG.

Evaluation of FLC-PEG-NP Hydrogel

Table 3 presents the values of pH measurement, FLC content, viscosity, homogeneity, and spreadability studies. The plain and FLC-PEG-NP hydrogels have nearly neutral pH values indicating the compatibility of these preparations with the rat skin. The prepared hydrogel containing FLC-PEG-NPs showed relatively high viscosity values compared to the blank hydrogel. This finding makes our formulation more suitable for drug release and local delivery. Regarding spreadability studies, medicated hydrogel showed a higher spreadability value of 6.4 ± 0.5 g.cm/s than that of plain hydrogel which may be due to the presence of PEG. On the other hand, both plain and FLC-PEG-NP hydrogels had good homogeneity and absences of any lumps, as they were uniform in consistency and free from any noticeable particulate matter after microscopic examination. The percentage of FLC content in the formed hydrogel was found to be satisfactory; with a mean content of 98.88 ± 3.9 which indicates the reproducibility of the FLC concentration in the prepared hydrogel.

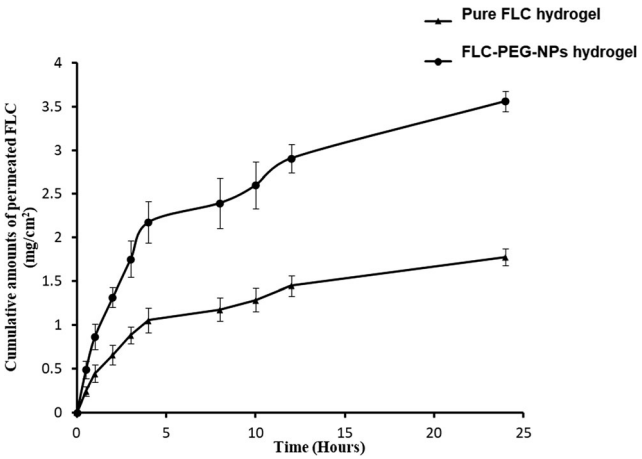

Fig. 7 Ex vivo permeation of drug from pure FLC-loaded hydrogel and FLC-PEG-NP-loaded hydrogel

In Vitro Drug Release

The in vitro release results of FLC from optimized FLC-PEG-NP hydrogel and hydrogel containing an equivalent amount of pure FLC preparations through a cellophane membrane were shown in Fig. 6 and represented as percent cumulative release against time. The release of pure drug form hydrogel was always lower than that from hydrogel containing drug in the form of optimized nanoparticles. The cumulative amounts of FLC released were calculated from FLC formulations, which showed a significantly higher FLC release ($p < 0.05$, ANOVA/Tukey tests) from the FLC-PEG-NP hydrogel where 83.22% of the loaded drug in the form of optimized FLC-PEG-NPs were released after 10 h compared to only about 42.51% of the loaded drug in the form of pure powder at the same time. The enhanced drug release from FLC-PEG-NP hydrogel could be attributed to the drug incorporated in the

Table 5 Antifungal activity of FLC using FLC powder and optimized FLC-PEG-NP hydrogel

Microorganisms	Zone of inhibition (mm)	
	FLC powder	FLC-PEG-NP hydrogel
Candida albicans	13.3 ± 1.3	19.5 ± 1.0
Candida glabrata	16.6 ± 0.3	25.4 ± 1.7
Epidermophyton floccosum	10.2 ± 1.2	14.1 ± 1.6
Trichophyton rubrum	12.1 ± 1.6	20.9 ± 2.7
Trichophyton verrucosum	16.0 ± 0.4	21.3 ± 1.4

hydrogel in the form of PEG-coated nanoparticles from which possess high water solubility than the FLC powder due to increased surface area. Also, the presence of PEG corona around the nanoparticles increases the FLC water solubility and consequently the release from the formulated hydrogel [19].

The kinetic analysis of drug release is indicated in Table 4 and it is obvious that the release of FLC from both plain and loaded hydrogel formulations obeys first-order release model. This finding means that as the soluble amount of FLC increases, the release rate increases and hence formulating the drug in the nanoparticles greatly increased the solubility and the release rate. The mechanism of release was found to be super case II transport.

Ex Vivo Permeation Study

The ex vivo permeation studies were conducted to give valuable information about the applicability of FLC-PEG-NP hydrogel product behavior in vivo (Fig. 7). The cumulative amount permeated of FLC across abdominal rat skin at 24 h post application of FLC-PEG-NP hydrogel was 3.45 ± 0.108 mg/cm^2. The amount of FLC permeated from the formulation was significantly higher in comparison to pure FLC containing hydrogel (1.650 ± 0.97 mg/cm^2) at p level < 0.05 by ANOVA/Tukey tests. The higher drug permeability from the FLC-PEG-NP hydrogel may be attributed to the partitioning of nanoparticles into stratum corneum. This better partitioning of FLC-PEG-NP hydrogel across stratum corneum in the deeper layers of skin under the influence of the transepidermal gradient could be considered one of the reasons for the better skin permeation of FLC-PEG-NPs. The above hypothesis was well supported by M. Kirjavainen et al. [25] who demonstrated that PEG molecules affect the stratum corneum lipid bilayer fluidity and improve drug partitioning.

Antifungal Activities

In order to confirm the release results, the antifungal activity of the prepared formulations was carried out. This study verified the local antifungal activity of FLC-PEG-NP hydrogel in comparison with pure FLC powder (as a positive control). Five strains of fungi were treated with FLC powder and the optimized FLC-PEG-NP hydrogel formulation. All the obtained results showed that the antifungal activity of FLC-PEG-NP hydrogel was better than that of pure powder. The statistical difference of the inhibition zone was investigated using one-way ANOVA followed by Tukey's post hoc test at probability (p) < 0.05. This finding could be as indicated by relatively high inhibition zone (Table 5). This higher antifungal activity of optimized FLC hydrogel formulation could be attributed to the higher water solubility of the drug in the form of nanoparticles and the penetrating power of PEG molecules which coated the fluconazole nanoparticles, and hence, higher diffusion into fungal wall. These results proved and confirmed the in vitro release results are recommended for further testing on the human volunteers.

Conclusion

Solvent antisolvent precipitation method was a successful method for the preparation of optimized PEG-coated FLC nanoparticles. The obtained nanoparticles were monodispersed, spherical in shape, and showed slight surface roughness. Good spreadability and homogeneity were observed with hydrogel loaded with fluconazole nanoparticles. Hydrogel containing optimized FLC-PEG-NPs exhibited higher drug release rate and also showed enhanced skin permeation compared with pure FLC-loaded hydrogel. The antifungal activity of FLC-PEG-NP-loaded hydrogel was significantly higher than pure drug-containing hydrogel. Development of hydrogel loaded with optimized polyethylene glycol-coated nanoparticles can be a promising delivery system for enhancing the local antifungal activity of fluconazole.

References

1. Algandaby MM, Al-Sawahli MM, Ahmed OAA, Fahmy UA, Abdallah HM, Hattori M, et al. Curcumin-zein nanospheres improve liver targeting and antifibrotic activity of curcumin in carbon tetrachloride-induced mice liver fibrosis. J Biomed Nanotechnol. 2016;12:1746–57.
2. Abou-Taleb HA, Hamd MA, Abdellatif AAH. Formulation of novel glycerin nanoparticles for enhancement the solubility of loratadine; application to transdermal hydrogel delivery system. J Nanomed Nanotechnol. 2017;8(2) Available from: https://www.omicsonline.org/open-access/formulation-of-novel-glycerin-nanoparticles-for-enhancement-thesolubility-of-loratadine-application-to-transdermal-hydrogel-delive-2157-7439-1000426.php?aid=85950
3. Bajaj A, Rao MRP, Pardeshi A, Sali D. Nanocrystallization by evaporative antisolvent technique for solubility and bioavailability enhancement of telmisartan. AAPS PharmaSciTech. 2012;13(4):1331–1340
4. Lonare AA, Patel SR. Antisolvent crystallization of poorly water soluble drugs. International Journal of Chemical Engineering and Applications. 2013;4(5):4:337–341.
5. Patel AP, Patel JK, Patel KS, Deshmukh AB, Mishra BR. A review on drug nanocrystal a carrier free drug delivery. Int J Res Ayurveda Pharm. 2011;2:448–58.
6. Sobue S, Sekiguchi K, Nabeshima T. Intracutaneous distributions of fluconazole , itraconazole , and griseofulvin in guinea pigs and

binding to human stratum corneum. Antimicrob Agents Chemother. 2004;48:216–23.
7. Pelaz B, del Pino P, Maffre P, Hartmann R, Gallego M, Rivera-Fernández S, et al. Surface functionalization of nanoparticles with polyethylene glycol: effects on protein adsorption and cellular uptake. ACS Nano. 2015;9:6996–7008. Available from https://doi.org/10.1021/acsnano.5b01326.
8. Salerno C, Carlucci AM, Bregni C. Study of in vitro drug release and percutaneous absorption of fluconazole from topical dosage forms. AAPS PharmSciTech [Internet]. 2010;11:986–93. Available from: http://www.springerlink.com/index/10.1208/s12249-010-9457-1
9. Hashem FM, Al-Sawahli MM, Nasr M, Ahmed OAA. Optimized zein nanospheres for improved oral bioavailability of atorvastatin. Int J Nanomedicine. 2015;10:4059–69.
10. Esnaashari SS, Amani A. Optimization of noscapine-loaded mPEG-PLGA nanoparticles and release study: a response surface methodology approach. J Pharm Innov. 2018;13(3):1–10.
11. Sahu BP, Das MK. Optimization of felodipine nanosuspensions using full factorial design. Int J PharmaTech Res. 2013;5:553–61.
12. Vaculikova E, Placha D, Pisarcik M, Peikertova P, Dedkova K, Devinsky F, et al. Preparation of risedronate nanoparticles by solvent evaporation technique. Molecules. 2014;19:17848–61.
13. Tawfeek HM. Novel gold nanoparticles coated with somatostatin as a potential delivery system for targeting somatostatin receptors. Drug Dev Ind Pharm. 2016;42(11):1782–91.
14. Abdellatif AAH, Tawfeek HM. Transfersomal nanoparticles for enhanced transdermal delivery of clindamycin. AAPS PharmSciTech. 2015;17. Available from: http://link.springer.com/10.1208/s12249-015-0441-7:1067–74.
15. Abdellatif AAH, Zayed GM, Kamel HH, Mohamed AG, Arafa WM, Khatib AM, et al. A novel controlled release microsponges containing Albendazole against Haemonchus contortus in experimentally infected goats. J Drug Deliv Sci Technol [Internet]. Elsevier; 2018;43:469–76. Available from: https://doi.org/10.1016/j.jddst.2017.10.022.
16. El-Feky GS, Farouk Abdulmaguid R, Zayed GM, Kamel R. Mucosal co-delivery of ketorolac and lidocaine using polymeric wafers for dental application. Drug Deliv [internet]. Informa Healthcare USA, Inc; 2018;25:35–42. Available from: https://www.tandfonline.com/doi/full/10.1080/10717544.2017.1413445.
17. Pillai O, Panchagnula R. Transdermal delivery of insulin from poloxamer gel: ex vivo and in vivo skin permeation studies in rat using iontophoresis and chemical enhancers. J Control Release. 2003;89:127–40.
18. Moazeni M, Kelidari HRHR, Saeedi M, Morteza-semnani K, Nabili M, Gohar AA, et al. Time to overcome fluconazole resistant Candida isolates: solid lipid nanoparticles as a novel antifungal drug delivery system. Colloids Surfaces B Biointerfaces [Internet]. Elsevier B.V.; 2016; Available from: https://doi.org/10.1016/j.colsurfb.2016.03.013.
19. El-feky GS, Zayed G, Farrag ARH. Optimization of an ocular nanosuspension formulation for acyclovir using factorial design. Int J Pharmcy Pharm Sci. 2013;5(1):213–219.
20. Gupta A, Aggarwal G, Singla S, Arora R. Transfersomes: a novel vesicular carrier for enhanced transdermal delivery of sertraline: development, characterization, and performance evaluation. Sci Pharm. 2012;80:1061–80.
21. Zayed GMS, Tessmar JKV. Heterobifunctional poly(ethylene glycol) derivatives for the surface modification of gold nanoparticles toward bone mineral targeting. Macromol Biosci [Internet]. WILEY-VCH Verlag; 2012;12:1124–36. Available from: https://doi.org/10.1002/mabi.201200046.
22. Gambhire M, Bhalekar M, Gambhire V. Statistical optimization of dithranol-loaded solid lipid nanoparticles using factorial design. Braz J Pharm Sci. 2011;47:503–11. Available from: http://www.scielo.br/scielo.php?pid=S1984-82502011000300008&script=sci_arttext
23. Devi Kusum V, Bhosale UV. Formulation and optimization of polymeric nano drug delivery system of acyclovir using 32 full factorial design. Int J PharmTech Res. 2009;1:644–53.
24. Dumont VC, Mansur AAP, Carvalho SM, Medeiros Borsagli FGL, Pereira MM, Mansur HS. Chitosan and carboxymethyl-chitosan capping ligands: effects on the nucleation and growth of hydroxyapatite nanoparticles for producing biocomposite membranes. Mater Sci Eng C [Internet]. Elsevier B.V. 2016;59:265–77. Available from: https://doi.org/10.1016/j.msec.2015.10.018
25. Kirjavainen M, Mönkkönen J, Saukkosaari M, Valjakka-Koskela R, Kiesvaara J, Urtti A. Phospholipids affect stratum corneum lipid bilayer fluidity and drug partitioning into the bilayers. J Control Release. 1999;58:207–14.